QCD with jets and photons at ATLAS and CMS

Jonathan Bossio - McGill University

on behalf of the ATLAS and CMS collaborations

MoriondQCD2019

La Thuile - 23–30 March 2019

The measurements presented here collectively probe:

- Precision QCD predictions (inclusive cross sections that probe PDFs and NLO QCD)
- Event topologies in interesting phase space regions (i.e. multijet production, dijet decorrelations, very forward region)
- Jet substructure (substructure observables, trimming and soft-drop, $g \rightarrow b\bar{b}$).

$\Delta\phi_{12}$ in nearly back-to-back jet topologies at $\sqrt{s} = 13$ TeV

Submitted to Eur. Phys. J. C, arXiv:1902.04374

Measurement performed in inclusive 2- and 3-jet events

- LO MCs: Pythia, Herwig++ and MadGraph+Pythia8
- NLO MCs: Powheg(2→2)+HERWIG++, Powheg(2→2)+Pythia8 and Powheg(2→3)+Pythia8
- Discrepancies with the unfolded data are as large as 15%, mainly in $177° < \Delta\phi_{12} < 180°$
- The 2- and 3-jet measurements are not simultaneously described by any of models

Inclusive 2-jet events

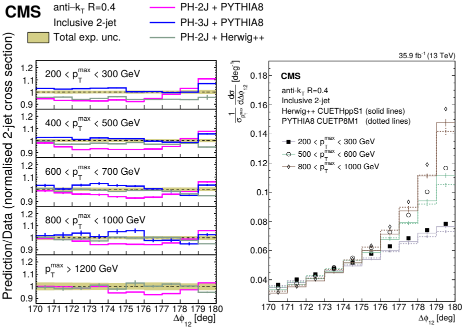

Inclusive 3-jet events

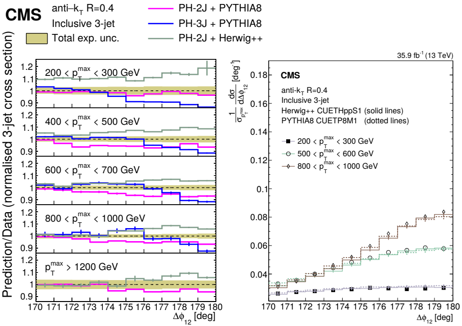

The two highest p_T jets must satisfy $|y| < 2.5$ and $p_T > 100\,\mathrm{GeV}$. For inclusive 3-jet events a third jet with $p_T > 30\,\mathrm{GeV}$ and $|y| < 2.5$ is required.

Azimuthal correlations in 2-, 3-, and 4-jet events at $\sqrt{s} = 13$ TeV

Eur. Phys. J. C 78 (2018) 566, arXiv:1712.05471

- $\Delta\phi_{2j}^{min}$: minimum azimuthal angles between any two of the three or four leading p_T jets
- NLO Herwig7 gives a better overall description than Powheg

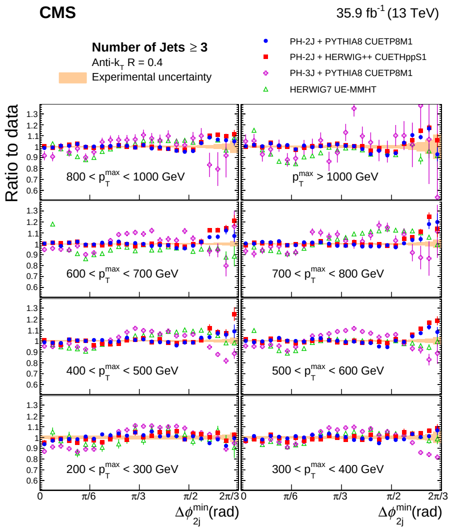

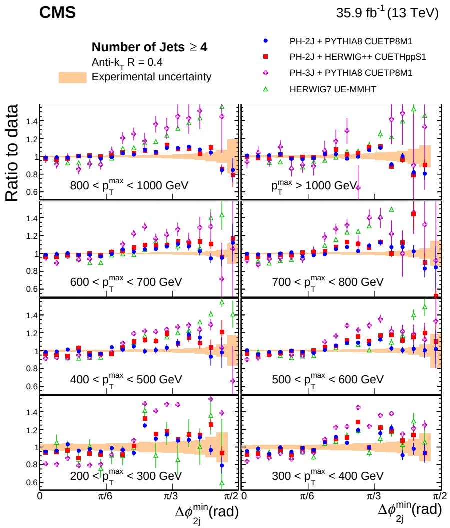

Dijet azimuthal decorrelations and α_s extraction at $\sqrt{s} = 8$ TeV

Phys. Rev. D 98 (2018) 092004, arXiv:1805.04691

Measurement of the rapidity and p_T dependence of dijet azimuthal decorrelations

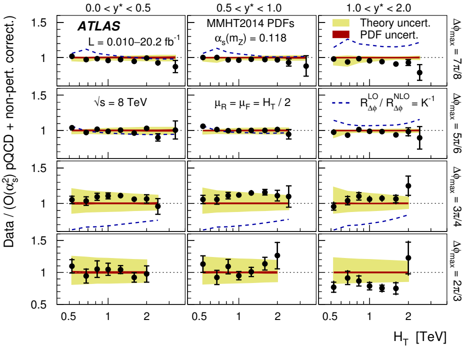

- $R_{\Delta\phi}$: fraction of dijet events w/ $\Delta\phi < \Delta\phi_{\max}$
- $R_{\Delta\phi}$ is measured as a function of the dijet rapidity interval y^*, the event total scalar transverse momentum H_T, and $\Delta\phi_{\max}$
- NLO pQCD predictions from NLOJET++, corrected for non-perturbative effects
- The theoretical predictions describe the unfolded data in the whole kinematic region

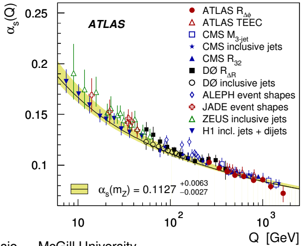

- Determination of α_s and its running
- Combination of the data at all momentum transfers results in $\alpha_s = 0.1127^{+0.0063}_{-0.0027}$

Inclusive very forward jet cross sections at $\sqrt{s_{NN}} = 5.02$ TeV

Submitted to J. High Energy Phys., arXiv:1812.01691

Cross sections are measured in proton-lead collisions as a function of jet energy

- Phase-space sensitive to the parton densities and their evolution at low fractional momenta
- Models incorporating various implementations of gluon saturation have been used
- Discrepancies btw. unfolded data and predictions of more than two orders of magnitude
- No model is currently able to describe all aspects of the data

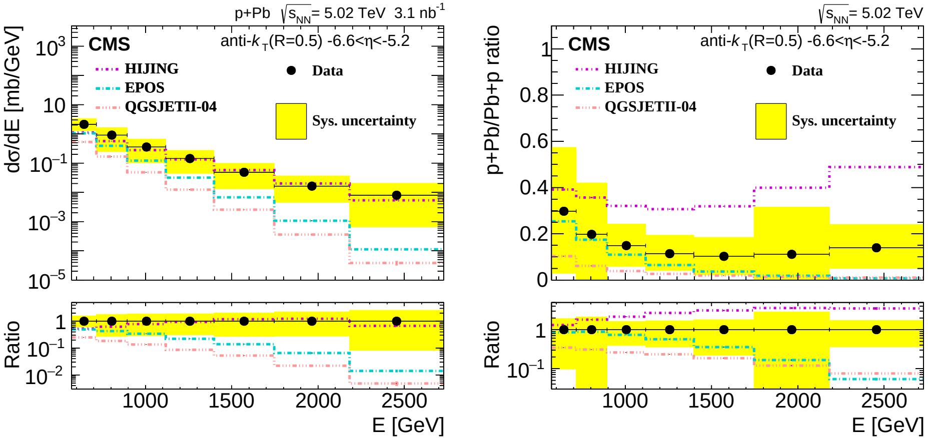

Event shape variables in multijet final states at $\sqrt{s} = 13$ TeV

J. High Energy Phys. 12 (2018) 117, arXiv:1811.00588

- Event shape variables (ESVs) are sensitive to the flow of energy in hadronic final states
- ESVs are measured in different $H_{T,2} = (p_{T\,\mathrm{jet1}} + p_{T\,\mathrm{jet2}})/2$ bins

The *complement of transverse thrust* is defined as $\tau_\perp \equiv 1 - T_\perp$ with $T_\perp \equiv \max_{\hat{n}_T} \frac{\sum_i |\vec{p}_{T,i} . \hat{n}_T|}{\sum_i p_{T,i}}$

$\tau_\perp$ is zero for a perfectly balanced two-jet event and is $1 - 2/\pi$ for an isotropic multijet event

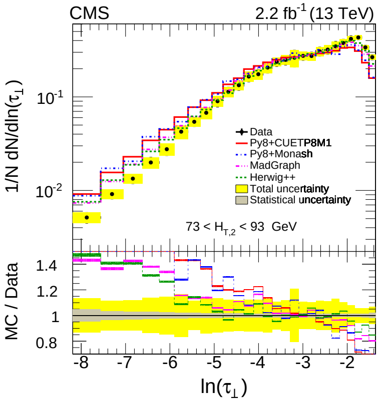

Higher $H_{T,2}$ $\Longrightarrow$

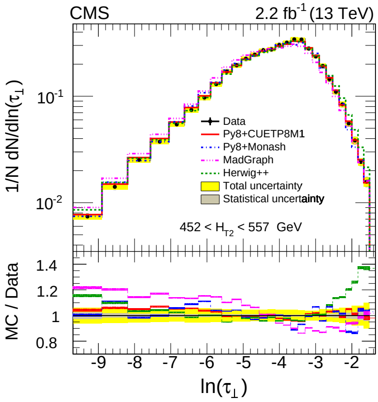

The agreement generally improves as $H_{T,2}$ increases

Measurement of the soft-drop jet mass at $\sqrt{s} = 13$ TeV

Phys. Rev. Lett. 121 (2018) 092001, arXiv:1711.08341

Measurement of the cross section as a function of $\log_{10}\rho^2$ in dijet events

Jet reclustering: $\frac{\min(p_{\mathrm{T}j_1}, p_{\mathrm{T}j_2})}{p_{\mathrm{T}j_1} + p_{\mathrm{T}j_2}} > \zeta_{\mathrm{cut}} \left(\frac{\Delta R_{12}}{R}\right)^{\beta}$

Smaller $\beta \rightarrow$ remove more soft particles

- $\rho \equiv m^{\text{soft drop}} / p_{\mathrm{T}}^{\text{ungroomed}}$

- Unfolded data is compared to MC simulation samples and pQCD calculations
- Bottom-up method to estimate (cluster-level) systematic uncertainties

LO+NNLL perform well for $\beta = 0 \Downarrow$

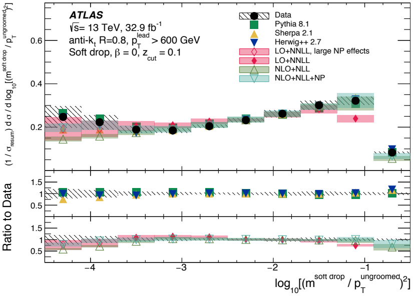

MC event generators better for higher $\beta \Downarrow$

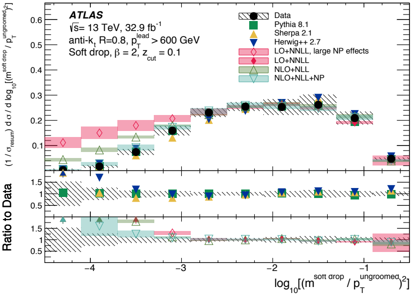

Measurement of jet substructure observables at $\sqrt{s} = 13$ TeV

Submitted to J. High Energy Phys., arXiv:1903.02942

Jet substructure observables in $t\bar{t}$ and inclusive jet events

- anti-k_t $R = 1.0$ jets groomed using two different techniques: trimming ($R_{\text{sub}} = 0.2$, $f_{\text{cut}} = 5\%$) and soft-drop ($\beta = 0, \zeta_{\text{cut}} = 0.1$)
- Unfolded data distributions are compared to various MC event generators
- Cluster-level uncertainties on the overall shape and scale of the observables

Observable: $D_2^{(\beta)} \equiv \dfrac{e_3^{(\beta)}}{\left(e_2^{(\beta)}\right)^3}$

$$e_n^{(\beta)} \equiv \frac{E_{\text{CF}n}(\beta)}{E_{\text{CF}1}(\beta)^n} \quad ; \quad E_{\text{CF}1}(\beta) \equiv \sum_{i \in J} p_{\mathrm{T}i}$$

$$E_{\text{CF}2}(\beta) \equiv \sum_{i<j \in J} p_{\mathrm{T}i} p_{\mathrm{T}j} (\Delta R_{ij})^\beta$$

$$E_{\text{CF}3}(\beta) \equiv \sum_{i<j<k \in J} p_{\mathrm{T}i} p_{\mathrm{T}j} p_{\mathrm{T}k} (\Delta R_{ij} \Delta R_{ik} \Delta R_{jk})^\beta$$

In general, reasonable agreement within uncertainties, with some discrepancies

Dijet selection

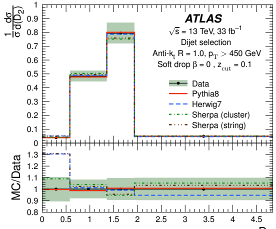

W selection

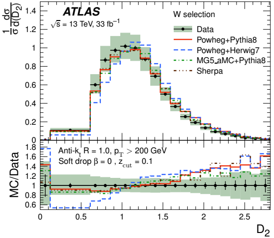

Properties of $g \to b\bar{b}$ at small opening angles at $\sqrt{s} = 13$ TeV

Submitted to Phys. Rev. D, arXiv:1812.09283

Main background source in analyses involving boosted Higgs decaying into *b*-quarks

- $R = 0.2$ anti-k_t jets from tracks are ghost-matched to $R = 1.0$ anti-k_t trimmed jets
- The contribution from $R = 1.0$ jets that don't have 2 track-jets containing B-hadrons is subtracted from data using template fits
- Unfolding to the particle level
- Significant differences observed b/w data and MC predictions

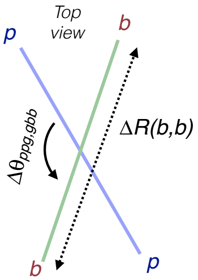

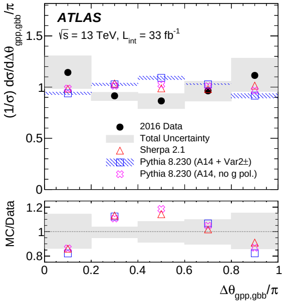

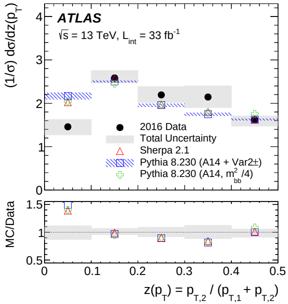

Inclusive isolated-photon and γ+jet cross sections at $\sqrt{s} = 13$ TeV

Eur. Phys. J. C 79 (2019) 20, arXiv:1807.00782

- Isolated-photon cross sections measured as a function of E_T^γ in different $|y^\gamma|$ bins
- γ+jet cross sections measured as a function of E_T^γ in different $|y^\gamma|$ and $|y^{jet}|$ bins
- Allows to test gluon PDF in different x and Q^2 values
- Prompt photons are identified with a boosted decision tree algorithm
- All measurements are in agreement with the NLO pQCD predictions

Inclusive isolated-photon cross section

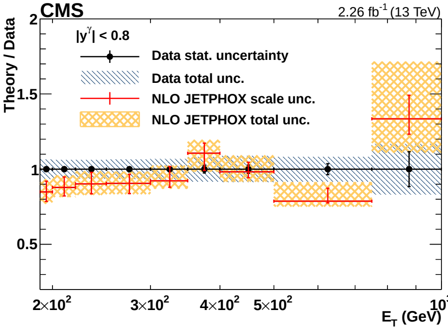

Photon+jet cross section

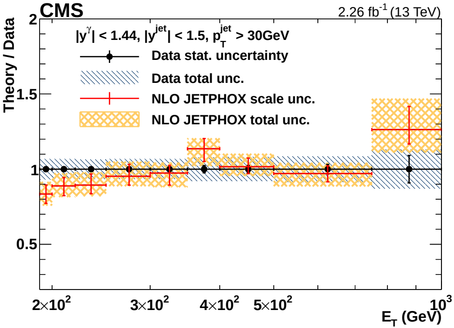

Ratio of inclusive isolated-γ cross sections at $\sqrt{s} = 8$ and 13 TeV

Submitted to J. High Energy Phys., arXiv:1901.10075

The ratio $(R^{\gamma}_{13/8})$ is measured as a function of the E_T^{γ} in different $|\eta^{\gamma}|$ ranges

- Reduced systematic and theoretical uncertainties by taking into account the correlations between the CMEs
- Photon energy scale is no longer the dominant uncertainty (with some exceptions at high E_T^{γ})
- A small background contribution still remains after imposing the photon identification and isolation requirements and is subtracted using a data-driven method
- NLO pQCD predictions calculated with JETPHOX are corrected for non-perturbative effects
- Predictions using several PDFs agree with the unfolded data within uncertainties

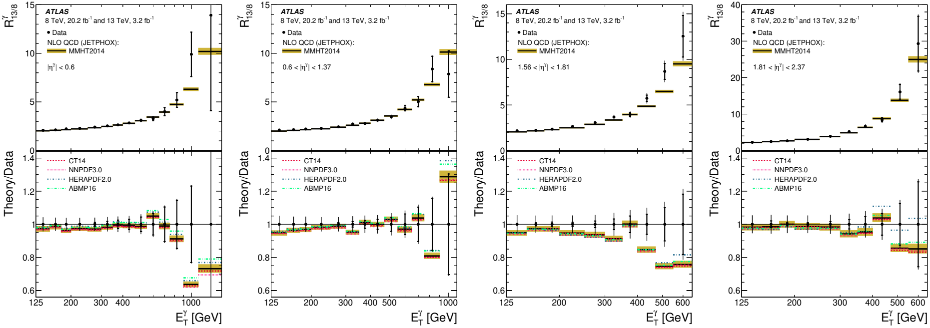

Isolated-photon plus jet production cross section at $\sqrt{s} = 13$ TeV

Phys. Lett. B 780 (2018) 578, arXiv:1801.00112

Isolated-photon plus jet cross-sections as a function of several observables

- Photons with $E_T^{\gamma} > 125$ GeV
- anti-k_t $R = 0.4$ jets with $p_T > 100$ GeV
- ME+PS@LO predictions from Sherpa and Pythia8 as well as NLO pQCD predictions from JETPHOX and Sherpa describe the data

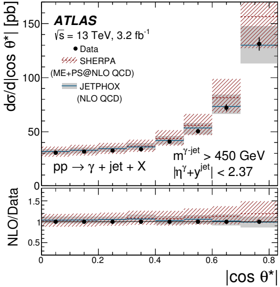

$\cos\theta^* \equiv \tanh(\Delta y/2)$ is sensitive to spin of exchange parton for $|\cos\theta^*| \to 1$

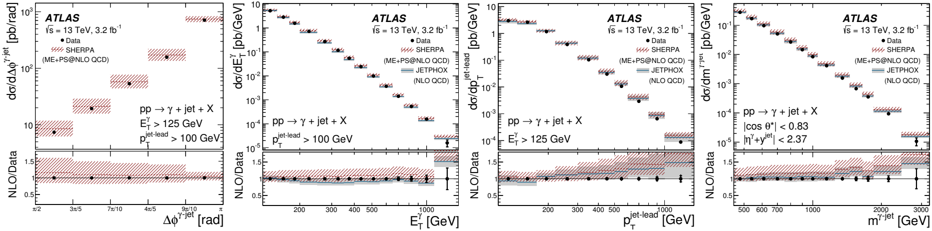

Conclusions

- Many great results from ATLAS and CMS experiments
- New interesting results for different phase spaces, jet substructure, and ratio of cross sections at different centre-of-mass energies
- Most of the results are well modelled by predictions
- Discrepancies are observed in some results
- Gives room to improve MC event simulations and pQCD predictions
- Huge effort made by performance groups to reduce experimental systematic uncertainties

Back-up slides

Monte Carlo event generators, parton densities, and underlying event tunes used for comparison with measurements

Matrix element generator	Simulated diagrams	PDF set	Tune
Pythia 8.219	2→2 (LO)	NNPDF2.3LO	CUETP8M1
Herwig++ 2.7.1	2→2 (LO)	CTEQ6L1	CUETHppS1
MadGraph+Pythia 8.219	2→2, 2→3, 2→4 (LO)	NNPDF2.3LO	CUETP8M1
PH-2J+Pythia 8.219	2→2 (NLO)	NNPDF3.0NLO	CUETP8M1
PH-2J+Herwig++ 2.7.1	2→2 (NLO)	NNPDF3.0NLO	CUETHppS1
PH-2J+Pythia 8.219	2→3 (NLO)	NNPDF3.0NLO	CUETP8M1

$\Delta\phi_{12}$ in nearly back-to-back jet topologies at $\sqrt{s} = 13$ TeV

Submitted to Eur. Phys. J. C, arXiv:1902.04374

Measurement performed in inclusive 2- and 3-jet events

- LO MCs: Pythia, Herwig++ and MadGraph+Pythia8
- NLO MCs: Powheg(2→2)+HERWIG++, Powheg(2→2)+Pythia8 and Powheg(2→3)+Pythia8
- Discrepancies with the unfolded data are as large as 15%, mainly in $177^\circ < \Delta\phi_{12} < 180^\circ$
- The 2- and 3-jet measurements are not simultaneously described by any of models

Inclusive 2-jet events

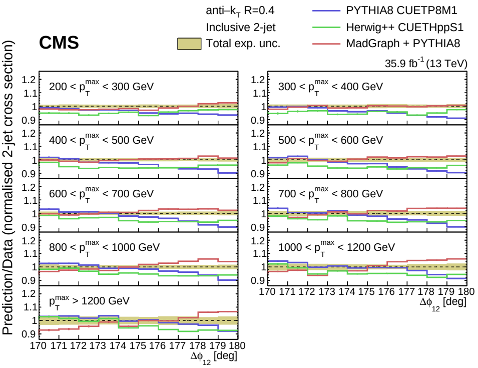

Inclusive 3-jet events

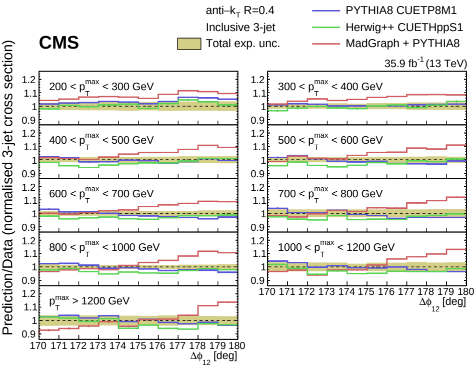

Azimuthal correlations in 2-, 3-, and 3-jet events at $\sqrt{s} = 13$ TeV

Eur. Phys. J. C 78 (2018) 566, arXiv:1712.05471

- $\Delta\phi_{2j}^{min}$: minimum azimuthal angles between any two of the three or four leading p_T jets

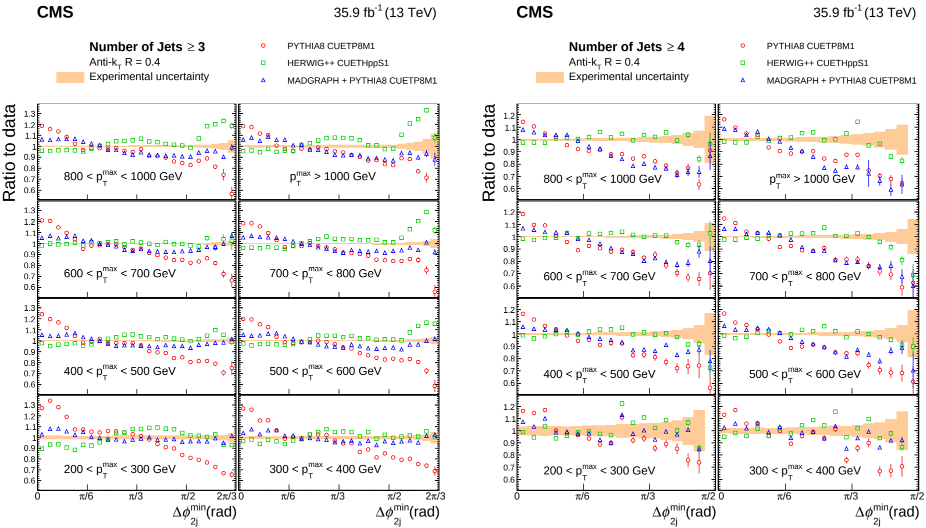

Monte Carlo event generators used for comparison in this analysis

Matrix element generator	Simulated diagrams	PDF set	Tune
PYTHIA 8.219 [9]	2→2 (LO)	NNPDF2.3LO [14, 15]	CUETP8M1 [13]
HERWIG++ 2.7.1 [10]	2→2 (LO)	CTEQ6L1 [16]	CUETHppS1 [13]
GRAPH5_aMC@NLO 2.3.3 [17, 18] + PYTHIA 8.219 [9]	2→2, 2→3, 2→4 (LO)	NNPDF2.3LO [14, 15]	CUETP8M1 [13]
POWHEG V2_Sep2016 [20–22] + PYTHIA 8.219 [9]	2→2 (NLO), 2→3 (LO)	NNPDF3.0NLO [28]	CUETP8M1 [13]
POWHEG V2_Sep2016 [20–22] + PYTHIA 8.219 [9]	2→3 (NLO), 2→4 (LO)	NNPDF3.0NLO [28]	CUETP8M1 [13]
POWHEG V2_Sep2016 [20–22] + HERWIG++ 2.7.1 [10]	2→2 (NLO), 2→3 (LO)	NNPDF3.0NLO [28]	CUETHppS1 [13]
HERWIG 7.0.4 [23]	2→2 (NLO), 2→3 (LO)	MMHT2014 [29]	H7-UE-MMHT [23]

The values of the parameters and the requirements that define the analysis phase space

Variable	Value
p_{Tmin}	100 GeV
$y_{\mathrm{boost}}^{\mathrm{max}}$	0.5
y^{*}_{max}	2.0
$p_{\mathrm{T1}}/H_{\mathrm{T}}$	$> 1/3$

Fit result for $\alpha_s\,(m_Z)$, determined from the $R_{\Delta\phi}$ data for $\Delta_{\phi_{\max}} = 7\pi/8$ with $0.0 < y^* < 0.5$ and $0.5 < y^* < 1.0$

$\alpha_{\mathrm{S}}(m_Z)$	Total uncert.	Statistical	Experimental correlated	Non-perturb. corrections	MMHT2014 uncertainty	PDF set	$\mu_{\mathrm{R,F}}$ variation
0.1127	${}^{+6.3}_{-2.7}$	± 0.5	${}^{+1.8}_{-1.7}$	${}^{+0.3}_{-0.1}$	${}^{+0.6}_{-0.6}$	${}^{+2.9}_{-0.0}$	${}^{+5.2}_{-1.9}$

All uncertainties have been multiplied by a factor of 10^3

Submitted to J. High Energy Phys., arXiv:1812.01691

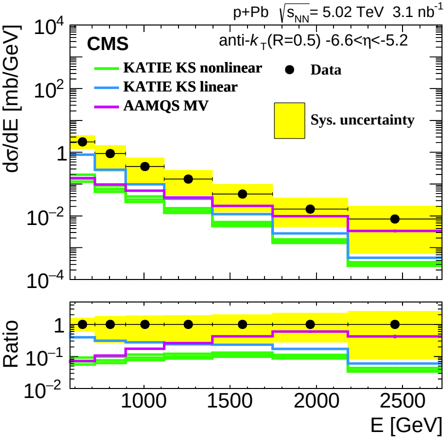

The contribution in percentage of various sources of systematic uncertainty in the highest and lowest common energy bins

	p+Pb		Pb+p		p+Pb/Pb+p	
Energy bin [TeV]	0.6	2.5	0.6	2.5	0.6	2.5
Energy scale	+2 −2	+150 −71	+1 −2	+120 −78	+1 −2	+35 −35
Model dependence	+18 −18	+41 −41	+4 −4	+60 −60	+1 −17	+47 −47
Alignment	+4 −4	+34 −34	+10 −10	+33 −33	+14 −3	+34 −6
Jet identification	+2 −2	+24 −24	+2 −2	<1 <1	<1 <1	+25 −25
Total	+19 −19	+160 −92	+11 −11	+140 −100	+27 −26	+77 −54

Event shape variables in multijet final states at $\sqrt{s} = 13$ TeV

J. High Energy Phys. 12 (2018) 117, arXiv:1811.00588

Event divided into upper (U) and lower (L) regions. Jets in U (L) satisfy $\vec{p}_{\mathrm{T},i}.\hat{n}_\mathrm{T} > 0$ (< 0)

The *total jet broadening* is defined as $B_\mathrm{Tot} \equiv B_\mathrm{U} + B_\mathrm{L}$, $B_\mathrm{X} \equiv \frac{1}{2P_\mathrm{T}} \sum_{i \in \mathrm{X}} p_{\mathrm{T},i} \sqrt{(\eta_i - \eta_\mathrm{X})^2 + (\phi_i - \phi_\mathrm{X})^2}$

$$\eta_X \equiv \frac{\sum_{i\in \mathrm{X}} p_{\mathrm{T},i}\eta_i}{\sum_{i\in \mathrm{X}} p_{\mathrm{T},i}}, \quad \phi_\mathrm{X} \equiv \frac{\sum_{i\in \mathrm{X}} p_{\mathrm{T},i}\phi_i}{\sum_{i\in \mathrm{X}} p_{\mathrm{T},i}},$$

and P_T is the scalar p_T sum of all jets in the event

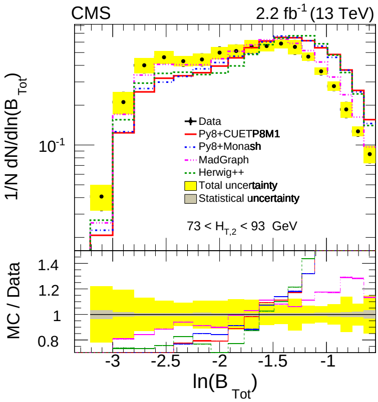

Higher $H_{T,2}$ $\Longrightarrow$

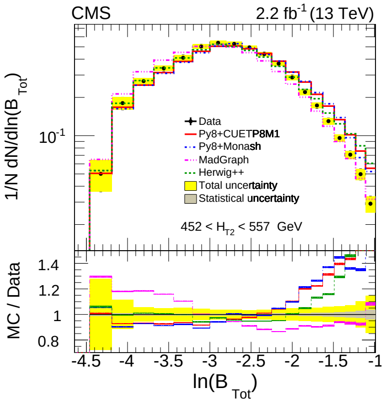

The agreement generally improves as $H_{T,2}$ increases

The normalized squared invariant mass of the jets in the U and L regions of the events is defined by:

$$\rho_{\mathrm{X}} \equiv \frac{M_{\mathrm{X}}^2}{P^2}$$

where M_{X} is the invariant mass jets in the region X, and P is the scalar sum of the momenta of all central jets

The *total jet mass* is defined as follows:

$$\rho_{\mathrm{Tot}} \equiv \rho_{\mathrm{U}} + \rho_{\mathrm{L}}$$

The *total transverse jet mass* $(\rho_{\mathrm{Tot}}^{\mathrm{T}})$ is similarly calculated using $\vec{p}_{\mathrm{T},i}$ of jets

Evolution of the mean of $\tau_{\perp}$, B_{Tot}, ρ_{Tot}, and ρ^{T}_{Tot} with increasing $H_{T,2}$

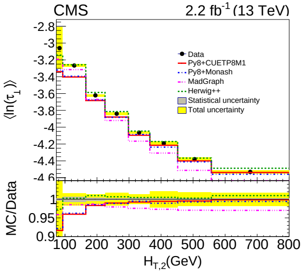

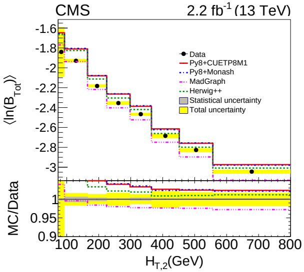

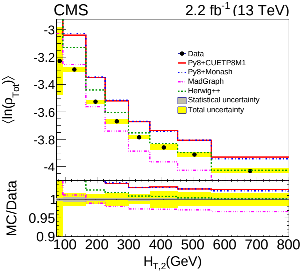

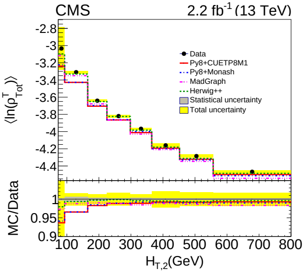

Measurement of the soft-drop jet mass at $\sqrt{s} = 13$ TeV

Phys. Rev. Lett. 121 (2018) 092001, arXiv:1711.08341

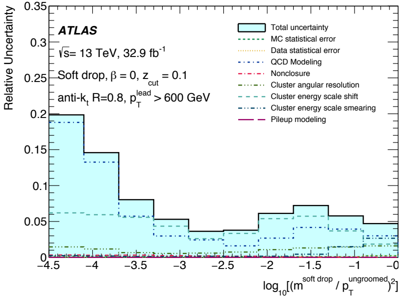

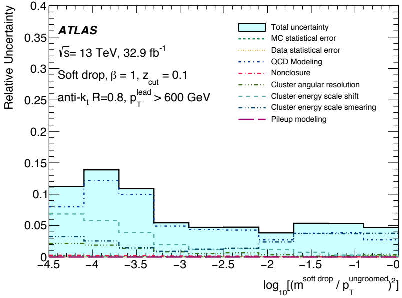

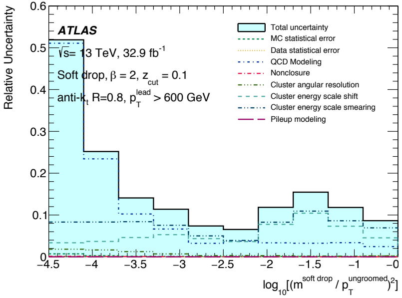

Measurement of the soft-drop jet mass at $\sqrt{s} = 13$ TeV

Phys. Rev. Lett. 121 (2018) 092001, arXiv:1711.08341

Measurement of the cross section as a function of $\log_{10}\rho^2$ in dijet events

Jet reclustering: $\frac{\min(p_{\mathrm{T}j_1}, p_{\mathrm{T}j_2})}{p_{\mathrm{T}j_1} + p_{\mathrm{T}j_2}} > \zeta_{\mathrm{cut}} \left(\frac{\Delta R_{12}}{R}\right)^{\beta}$

Smaller $\beta \rightarrow$ remove more soft particles

- $\rho \equiv m^{\text{soft drop}} / p_{\mathrm{T}}^{\text{ungroomed}}$
- Unfolded data is compared to MC simulation samples and pQCD calculations
- Bottom-up method to estimate (cluster-level) systematic uncertainties
- LO+NNLL perform well for $\beta = 0 \Longrightarrow$
- MC event generators better for higher $\beta \Downarrow$

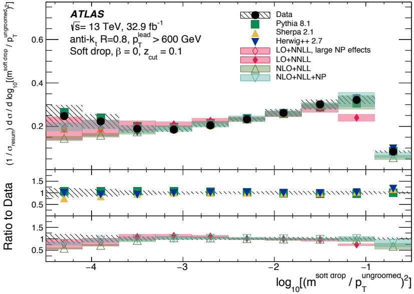

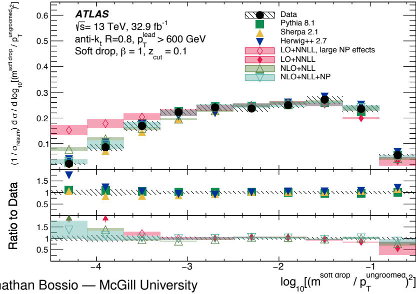

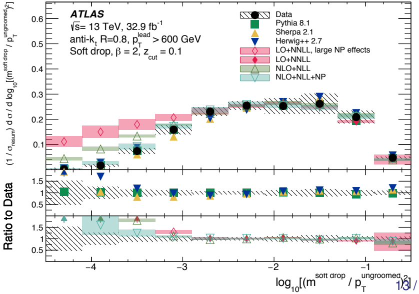

Jet substructure observables in $t\bar{t}$ and inclusive jet events

- anti-k_t $R = 1.0$ jets groomed using two different techniques: trimming ($R_{\text{sub}} = 0.2$, $f_{\text{cut}} = 5\%$) and soft-drop ($\beta = 0$, $\zeta_{\text{cut}} = 0.1$)
- Unfolded data distributions are compared to various MC event generators
- Cluster-level uncertainties on the overall shape and scale of the observables

$$e_n^{(\beta)} \equiv \frac{E_{\text{CF}n}(\beta)}{E_{\text{CF}1}(\beta)^n} \quad ; \quad E_{\text{CF}1}(\beta) \equiv \sum_{i \in J} p_{\text{T}i}$$

$$E_{\text{CF}2}(\beta) \equiv \sum_{i<j \in J} p_{\text{T}i} p_{\text{T}j} (\Delta R_{ij})^\beta$$

$$E_{\text{CF}3}(\beta) \equiv \sum_{i<j<k \in J} p_{\text{T}i} p_{\text{T}j} p_{\text{T}k} (\Delta R_{ij} \Delta R_{ik} \Delta R_{jk})^\beta$$

Observable: $D_2^{(\beta)} \equiv \dfrac{e_3^{(\beta)}}{\left(e_2^{(\beta)}\right)^3}$

In general, reasonable agreement within uncertainties, with some discrepancies

Dijet selection

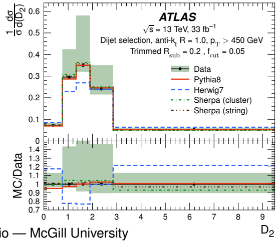

W selection

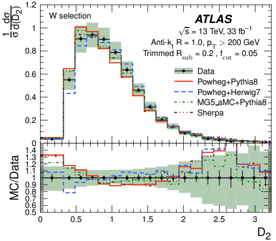

Summary of systematic uncertainty sizes for each observable for the normalized differential cross sections

	$\Delta R(b,b)$	$\Delta\theta_{\text{ppg,gbb}}$	$z(p_{\text{T}})$	$\log(m_{bb}/p_{\text{T}})$
Calorimeter jet energy	2–3%	2–3%	2–6%	2–4%
Flavor tagging	<1%	<1%	<1%	<1%
Tracking	1–2%	1–2%	2–4%	1–2%
Background fit	1%	1%	1–2%	2%
Unfolding method	2–3%	2%	2–4%	2–5%
Theoretical modeling	3–10%	2–13%	3–10%	4–11%
Statistical	1%	1%	2%	1%
Total	3–10%	3–10%	3–14%	4–12%

Properties of $g \rightarrow b\bar{b}$ at small opening angles at $\sqrt{s} = 13$ TeV

Submitted to Phys. Rev. D, arXiv:1812.09283

- The contribution from large-R jets that do not have two associated track-jets containing B-hadrons is subtracted from data, before correcting for detector effects
- Correction factors are determined from data template fits to the signed impact parameter distribution (s_{d_0}) and applied for each bin of the four observables
- In each bin, the distribution of s_{d_0} is fitted to data using templates from simulation while letting the fraction of each flavor component float in the fit.
- For a given track, $s_{d_0} = s_j |d_0| / \sigma(d_0)$, where d_0 is the transverse impact parameter relative to the beam-line, $\sigma(d_0)$ is the uncertainty in d_0 from the track fit, and the variable s_j is the sign of d_0 with respect to the jet axis: $s_j = +1$ if $\sin(\phi_{\text{jet}} - \phi_{\text{track}}) \cdot d_0 > 0$ and $s_j = -1$ otherwise.

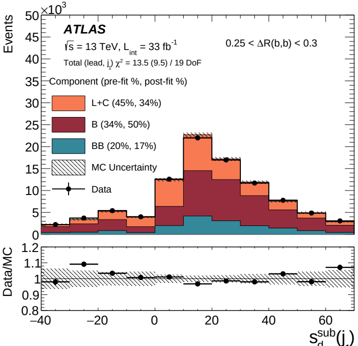

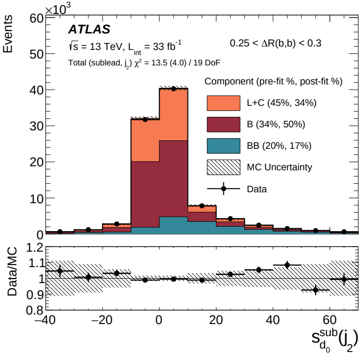

Properties of $g \to b\bar{b}$ at small opening angles at $\sqrt{s} = 13$ TeV

Submitted to Phys. Rev. D, arXiv:1812.09283

Main background source in analyses involving boosted Higgs decaying into *b*-quarks

- $R = 0.2$ anti-k_t jets from tracks are ghost-matched to $R = 1.0$ anti-k_t trimmed jets
- The contribution from $R = 1.0$ jets that don't have 2 track-jets containing B-hadrons is subtracted from data using template fits
- Unfolding to the particle level
- Significant differences observed b/w data and MC predictions

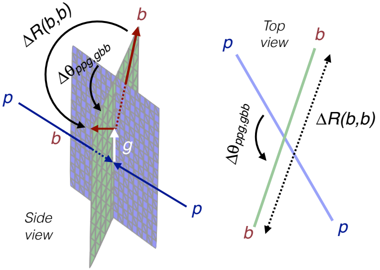

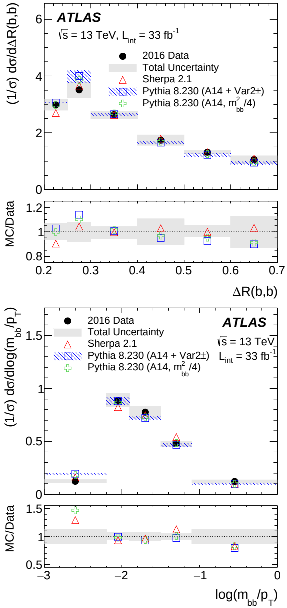

Impact on cross sections, in percent, for each systematic uncertainty source
(The ranges, when quoted, indicate the variation over photon ET between 190-1000 GeV)

Source	$\lvert y^\gamma \rvert < 0.8$	$0.8 < \lvert y^\gamma \rvert < 1.44$	$1.57 < \lvert y^\gamma \rvert < 2.1$	$2.1 < \lvert y^\gamma \rvert < 2.5$
Trigger efficiency	0.7–8.5	0.2–13.4	0.6–20.5	0.3–7.8
Selection efficiency	0.1–1.3	0.1–1.3	0.1–5.3	0.1–1.1
Data-to-MC scale factor	3.7	3.7	7.1	7.1
Template shape	0.6–5.0	0.1–10.2	0.5–4.9	0.6–16.2
Unfolding	3.8–5.5	1.2–4.1	2.0–8.5	2.3–10.3
Total w/o luminosity	5.4–12.0	5.9–18.2	8.2–26.9	8.6–21.7
Integrated luminosity	2.3			

Ratio of inclusive isolated-γ cross sections at $\sqrt{s} = 8$ and 13 TeV

Submitted to J. High Energy Phys., arXiv:1901.10075

Relative theoretical uncertainty in $R^{\gamma}_{13/8}$ as a function of E^{γ}_{T} for different $|\eta^{\gamma}|$ regions

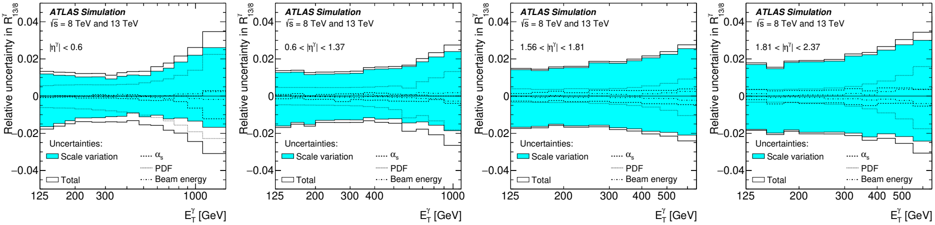

Relative systematic uncertainty in $R^{\gamma}_{13/8}$ as a function of E^{γ}_{T} for different $|\eta^{\gamma}|$ regions

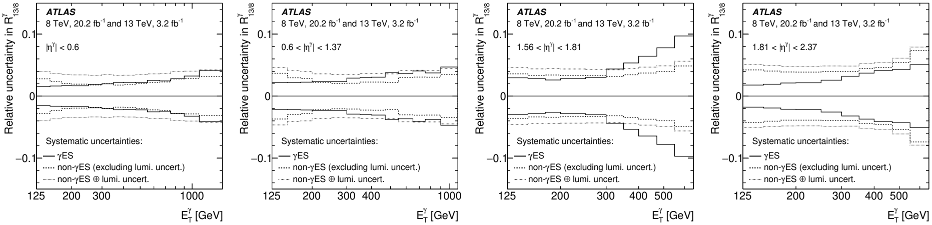

Ratio of inclusive isolated-γ cross sections at $\sqrt{s} = 8$ and 13 TeV

Submitted to J. High Energy Phys., arXiv:1901.10075

Total relative systematic uncertainty in $R^{\gamma}_{13/8}$ as a function of E_T^{γ} for different $|\eta^{\gamma}|$ regions

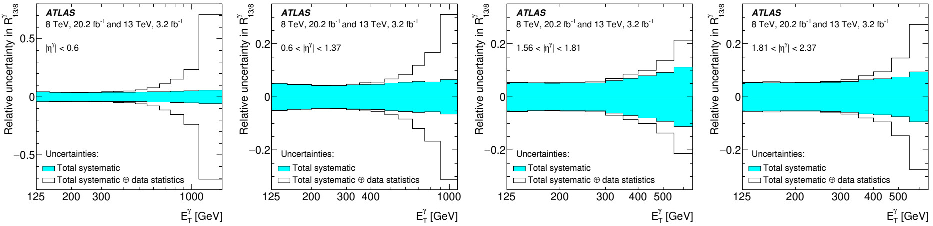

Theoretical uncertainties in $R^{\gamma}_{13/8}$:

- The uncertainties due to the PDFs, α_s, beam energy and non-perturbative effects are fully correlated between the two centre-of-mass energies
- The relative uncertainty in $R^{\gamma}_{13/8}$ due to the uncertainties in α_s, the PDFs and the beam energy are significantly smaller with respect to the individual predictions
- However, for the scale uncertainties, the correlation is a priori unknown
- Varying the scales coherently or incoherently at both centre-of-mass energies leads to very different uncertainties
- A second approach is also investigated, which is free from ambiguity in the correlation. It consists of considering the difference between the LO and NLO predictions for $R^{\gamma}_{13/8}$.
- The results of this second approach support the use of coherent variations of the scales; an incoherent variation of the scales leads to an overestimation of the theoretical uncertainty.

Ratio of inclusive isolated-γ cross sections at $\sqrt{s} = 8$ and 13 TeV

Submitted to J. High Energy Phys., arXiv:1901.10075

Experimental uncertainties in $R^{\gamma}_{13/8}$:

- A proper estimation of the systematic uncertainties requires taking into account inter-$\sqrt{s}$ correlations for each source of systematic uncertainty.
- Assuming no correlation provides a conservative estimate and full correlation is used only when justified.
- The uncertainty arising from the γ energy scale is estimated by decomposing it into uncorrelated sources for both the 8 and 13 TeV measurements
- A total of 22 individual components are considered
- Twenty of these components are common to both centre-of-mass energies
- The remaining two components are specific to the 13 TeV measurement
- All the components are taken as fully correlated except for the uncertainty in the overall energy scale adjustment using $Z \to e^+e^-$ events, which for 2015 includes the effects of the changes in the configuration of the ATLAS detector, and the uncertainties specific to the 13 TeV measurement
- The uncertainties due the γ energy resolution are treated as uncorrelated between $\sqrt{s} = 13$ TeV and 8 TeV since they include the effects of pile-up, which was different in the 2012 and 2015 data-taking periods
- Other sources of uncertainty are treated as uncorrelated

Submitted to J. High Energy Phys., arXiv:1901.10075

- In addition, the $R^{\gamma}_{13/8}$ ratio to that of the fiducial cross sections for Z boson production at 13 and 8 TeV using the decay channels $Z \to e^+e^-$ and $Z \to \mu^+\mu^-$ is made and compared with the theoretical predictions
- In this double ratio, a further reduction of the experimental uncertainty is obtained because the uncertainties arising from the luminosity measurement cancel out
- The predictions describe the measurements of the double ratio within the theoretical and experimental uncertainties

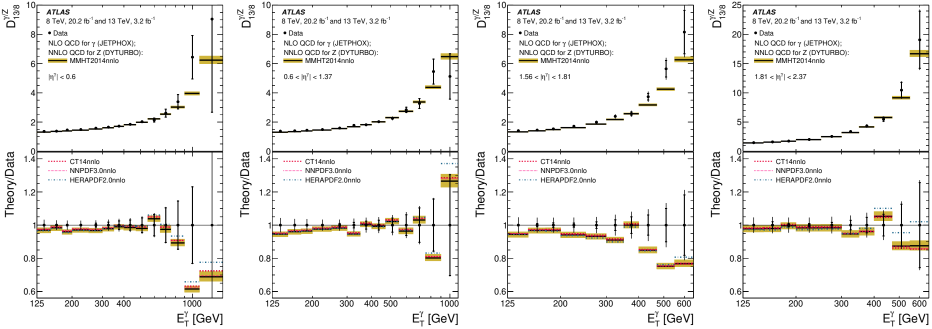

Isolated-photon plus jet cross-sections as a function of several observables

- Photons with $E_T^{\gamma} > 125\,\mathrm{GeV}$
- anti-k_t $R = 0.4$ jets with $p_T > 100\,\mathrm{GeV}$
- ME+PS@LO predictions from Sherpa and Pythia8 as well as NLO pQCD predictions from JETPHOX and Sherpa describe the data

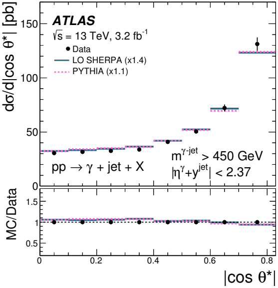

$\cos\theta^* \equiv \tanh(\Delta y/2)$ is sensitive to spin of exchange parton for $|\cos\theta^*| \to 1$

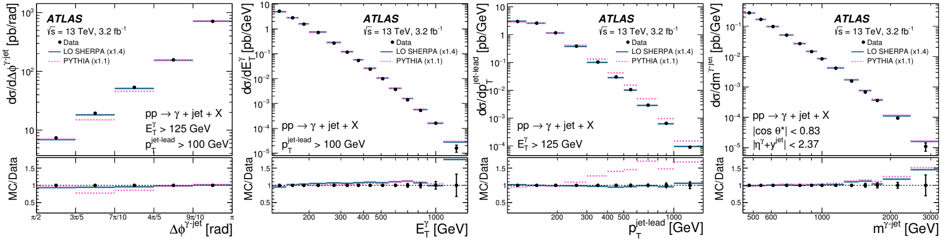

Isolated-photon plus jet production cross section at $\sqrt{s} = 13$ TeV

Phys. Lett. B 780 (2018) 578, arXiv:1801.00112

Requirements on photons

$E_T^\gamma > 125$ GeV, $|\eta^\gamma| < 2.37$ (excluding $1.37 < |\eta^\gamma| < 1.56$)

$E_T^{\text{iso}} < 4.2 \cdot 10^{-3} \cdot E_T^\gamma + 10$ GeV

Requirements on jets

anti-k_t algorithm with $R = 0.4$

the leading jet within $|y^{\text{jet}}| < 2.37$ and $\Delta R^{\gamma-\text{jet}} > 0.8$ is selected

$p_T^{\text{jet-lead}} > 100$ GeV

UE subtraction using $k_\perp$ algorithm with $R = 0.5$ (cf. Section ??)

Additional requirements for $d\sigma/dm^{\gamma-\text{jet}}$ and $d\sigma/d|\cos\theta^*|$

$|\eta^\gamma + y^{\text{jet-lead}}| < 2.37$, $|\cos\theta^*| < 0.83$ and $m^{\gamma-\text{jet}} > 450$ GeV